

Vibration Analysis and Modelling of Light-weight Robot Arms

Ryszard LENIOWSKI¹ , Michał WRÓŃSKI² 

^{1,2} Rzeszów University of Technology, al. Powstańców Warszawy 12

Corresponding author: Ryszard LENIOWSKI, email: lery@kia.prz.edu.pl

Abstract Lightweight robots (LWR) are a new generation of devices intended to be used not only for industrial tasks but also to perform actions in the human environment. This work presents an analysis of selected basic problems related to the vibration properties of light-weight robot arms. The study of vibration is based on the analysis of the root locus on the plane of complex variables. It turns out that their distribution is non-stationary and depends on the parameters of the model (arm geometry, material parameters), but also depends on the type of realised motion, which is not so obvious. Depending on the manoeuvres conducted (acceleration / deceleration), the system may lose (or increase) its oscillating properties at higher frequencies, as well as introduce a structural (measurable) delay. Recognition of the discussed properties along with their modelling is an important element of the design process of the control system of modern, light-weight robots.

Keywords: flexible deformation, vibration analysis, light-weight robots.

1. Introduction

The problem of mathematical modelling of light robots is one of the most important considering the wide range of their applications. The diagram in Fig. 1 takes into account only those types of models that are related to the considered problem. We see that the degree of connection between them varies. Each group has many representations (subgroups), which can be seen in the example of the dynamics model. In addition, the remaining groups of models may have many representations, usually differing in the degree of complication.

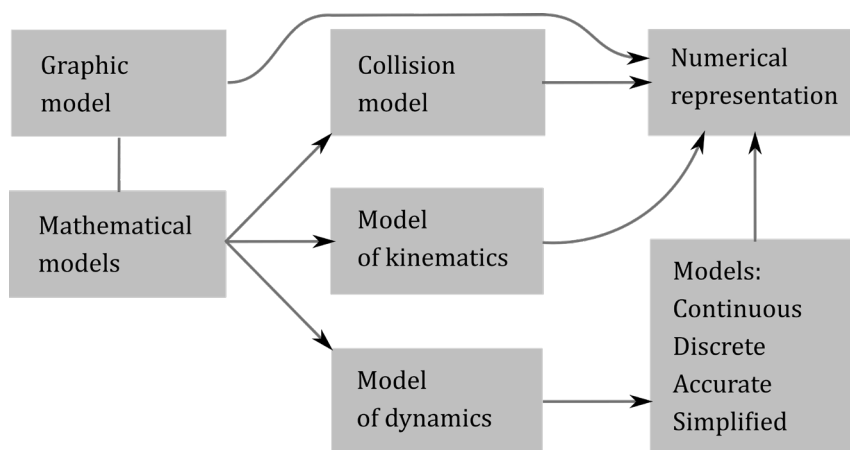


Figure 1. Types of mathematical models of LWR.

The study of the LWR vibration damping process focuses on dynamics models. The problem of describing the dynamics of flexible structures was studied by eminent mathematicians (L. Euler), and later mechanics (S. Timoshenko), long before the advent of robotics. W. Book [8], who was the first to introduce the concept of "flexible manipulators", should be considered a precursor to research on robots with flexible arms. Using a complex mathematical apparatus and specialized, dedicated software, many partial problems were solved over a period of two decades [1-2,4], but due to the high level of complexity of such objects, issues remain open.

More and more precise representations of the models shown in Fig.1 are sought, especially dynamics models. The problem of determining the dynamics model begins with indicating the class of the model that we want to determine. Two classes of models are assumed: the first are "accurate" models, generated for simulation purposes. They are systems of highly non-linear ordinary or partial differential equations that describe the dynamics of beams or shells. When creating such a model, the aim is to approximate the real system as much as possible by using the most commonly known formalisms, e.g. Lagrange, in conjunction with a symbolic computation processor. The second class consists of "simplified" models, used at the stage of synthesis of control systems or visualization of the tested object. In this case, the aim is to obtain a model that is as simple as possible. Certain reduction and simplification methods are adopted, which lead to the obtaining of the dynamics model as a linear, partial differential equation of the parabolic type or its reduced form, i.e. a finite-dimensional system in a continuous or discrete (with respect to time) version. FEM (Finite Element Method) [3] models with varying levels of accuracy are also used. In analytical models, additional correction terms are often introduced, which bring the model spectrum closer to the real system spectrum.

The expected quality of the model, which consists of the accuracy (as high as possible) and the level of complication (as low as possible), has influence on the selection of the spatial transformations used to describe the deformation process.

2. Model selection - discussion

The discussion of the choice of the model describing the deformation of the arm is one of the issues related to the mathematical modelling of light robots. Due to their complexity and degree of interconnection, new design and simulation methods are sought for such complex mechatronic systems.

We derive the LWR dynamics equations using the Lagrange formalism and the transverse deformation model. The form of the model depends on the choice of a combination of movements (non-distortion transformations) and deformations, the result of which is the inclusion in the analysis of the corresponding component of kinetic and potential energy. The types of transformation and the corresponding models are presented in Table 2.2. The symbol "+" means that an energy component is included in the model, while the symbol "-" means that it is not.

Table 1. Types of deformation and corresponding models.

Model	Potential energy			Kinetic energy		
	Translation	Rotation	Shear	Translation	Rotation	Shear
Euler-Bernoulli	+	-	-	+	-	-
Rayleigh	+	-	-	+	+	-
No-name	+	-	+	+	-	-
Timoshenko	+	+	+	+	+	-

The given table shows that it is possible to create other models that would include further "energy fixes". Selected types of deformation and corresponding models are presented in [5], [9] and [10]. When improving the model, one should remember its complexity so that it is useful in research. Table 1 corresponds to the potential and kinetic energies. In further considerations, we will apply simplifications in the notation of formulas consisting in omitting the arguments representing spatial variables and time, marking e.g. $w(x, t)$ as w .

2.1. Euler-Bernoulli model (EBM)

Assuming that the distributed perpendicular force f acts on the arm, the solution of the Lagrange equation leads to the well-known [2] model of dynamics:

$$\rho A \frac{\partial^2 w(x,t)}{\partial t^2} + EI \frac{\partial^4 w(x,t)}{\partial x^4} = f(x, t). \quad (1)$$

The solution (1) with boundary conditions (one end clamped, the other free) is based on the separation of variables (we assume that $w(x,t)=W(x)T(t)$) and the theory of linear operators. The roots of the characteristic equation (for clamped-free) form an infinite sequence of two conjugated pairs:

$$s_{1,2} = \mp \sqrt[4]{\omega^2 \frac{\rho A}{EI}} \quad \text{and} \quad s_{3,4} = \mp i \sqrt[4]{\omega^2 \frac{\rho A}{EI}} \quad (2)$$

Comparing the experimental and theoretically determined modes of natural vibrations, it turns out that the EBM model overestimates them by (14% - 26%) for the first mode and by (78% - 133%) for the second mode of vibrations. The error increases at higher frequencies. For this reason, it is now used less frequently.

2.2. Rayleigh model (RM)

As mentioned in the discussion of model selection, the Rayleigh beam adds rotary inertia effects to the Euler-Bernoulli beam. Hence, equation (3) contains three terms on the left:

$$EI \frac{\partial^4 w}{\partial x^4} - \rho I \frac{\partial^4 w}{\partial x^2 \partial t^2} + \rho A \frac{\partial^2 w}{\partial t^2} = f(x, t). \tag{3}$$

By proceeding analogously to the EBM model and passing from the time form to the Laplace operator domain, the characteristic equation is obtained as:

$$EIs^4 + \rho I \omega^2 s^2 - \rho A \omega^2 = 0. \tag{4}$$

The roots of the characteristic equation (for the same boundary conditions for the EBM model) are more complex compared to (2) and are equal:

$$s_{1,2} = \pm i \sqrt{\rho I \frac{\omega^2}{2} + \omega \sqrt{I \frac{\rho^2 \omega^2}{4} + \rho A}} \tag{5}$$

and

$$s_{3,4} = \pm \sqrt{-\rho I \frac{\omega^2}{2} + \omega \sqrt{I \frac{\rho^2 \omega^2}{4} + \rho A}}.$$

The deviations from the experimental model are (1% - 7%) and (5% - 16%) for the first and second modes of vibration, respectively.

2.3. Timoshenko model (TM)

According to Table 1, the kinetic energy of the TM model is a sum of the kinetic energy for translational motion and rotational motion (as a result of torsional deformation and two deflections). The potential energy of elasticity consists of the energy of deflection and shear deformation. Assuming some simplifications (with respect to zero energy dissipation and generalized zero external excitation limited to force p and torque q), the TM model in a homogeneous form for zero inputs (distributed force p = 0, distributed moment q = 0) consists of two equations corresponding to the variables w(x,t) and φ(x,t):

$$\begin{cases} EI \frac{\partial^4 w}{\partial x^4} - \left(\rho I + \frac{\rho}{GAK_s}\right) \frac{\partial^4 w}{\partial x^2 \partial t^2} + \rho A \frac{\partial^2 w}{\partial t^2} + \frac{\rho^2 I}{GAK_s} \frac{\partial^4 w}{\partial t^4} = 0 \\ EI \frac{\partial^4 \varphi}{\partial x^4} - \left(\rho I + \frac{\rho}{GAK_s}\right) \frac{\partial^4 \varphi}{\partial x^2 \partial t^2} + \rho A \frac{\partial^2 \varphi}{\partial t^2} + \frac{\rho^2 I}{GAK_s} \frac{\partial^4 \varphi}{\partial t^4} = 0 \end{cases} \tag{6}$$

We note that the above equations have an identical form; therefore, their solutions will be similar and will depend on the boundary conditions and natural vibrations. To obtain the characteristic equation, the variable separation should be introduced. The analysis is carried out conveniently for the dimensionless coordinate ξ = x / L. We assume that w(x, t)=W(ξ)e^{iωt} and φ(x, t)=φ(ξ) e^{iωt}. By inserting new variables into (6) we get (7) consist of two equations corresponding to the variables w(x,t) and φ(x,t):

$$\begin{cases} W'''' + \left(\rho I + \frac{\rho}{GAK_s}\right) \omega^2 W'' + \left(\frac{\rho^2 I}{GKA_s} \omega^4 - \rho A \omega^2\right) W = 0 \\ \phi'''' + \left(\rho I + \frac{\rho}{GAK_s}\right) \omega^2 \phi'' + \left(\frac{\rho^2 I}{GKA_s} \omega^4 - \rho A \omega^2\right) \phi = 0 \end{cases} \tag{7}$$

The characteristic equation has the form:

$$EIs^4 + \left(\rho I + \frac{\rho}{GAK_s}\right) \omega^2 s^2 + \left(\frac{\rho^2 I}{GKA_s} \omega^4 - \rho A \omega^2\right) = 0. \tag{8}$$

The solution (8) is the four elements grouped in pairs:

$$s_{1,2} = \mp i \sqrt{\rho \left(\rho I + \frac{\rho}{GAK_s}\right) \frac{\omega^2}{2} + \omega \sqrt{\left(I - \frac{1}{GAK_s}\right) \frac{\rho^2 \omega^2}{4} + \rho A}} \tag{9}$$

and

$$s_{3,4} = \mp \sqrt{-\rho \left(I + \frac{1}{GAK_s} \right) \frac{\omega^2}{2} + \omega \sqrt{\left(I - \frac{1}{GAK_s} \right) \frac{\rho^2 \omega^2}{4} + \rho A}} \tag{10}$$

Analysing the formulas (8, 9), it is easy to notice that the first two roots will always be imaginary. On the other hand, the two remaining elements (formula 10) will take either real or imaginary values, depending on the value of the pulsation ω , the limiting value of which is $\omega = \sqrt{GAK_s/\rho I}$. Comparing the experimental and theoretically determined vibration modes, it turns out that for the TM-type models, the deviations are respectively: -1% to 2% for the first mode of vibration, and -1% to 6% for the second [5-6]. This is a significantly better result compared to the EBM model. The disadvantage of the model, however, is its complexity and its inability to take into account rheological properties. The complication of the model hinders the discretization process to such an extent that some researchers consider the RM model to be sufficiently accurate, when the energy dissipation is added.

3. Rayleigh model with damping and axial force (RDFM)

For low pulsations, the internal damping depends mainly on the stress level in the material and is non-linear. Linear rheological models can be used for low and medium stresses, and such stresses occur most frequently during robot operation. The Kelvin-Voigt model seems to be the most useful due to its simplicity and sufficient accuracy. The relationship between stress σ and the strain ϵ for this model is as follows:

$$\sigma = E\epsilon + 2\mu E\dot{\epsilon} \tag{11}$$

The inclusion of rheological properties and axial forces significantly brings model (12) closer to the real system:

$$EI \frac{\partial^4 w}{\partial x^4} + 2\mu EI \frac{\partial^5 w}{\partial x^4 \partial t} - \rho I \frac{\partial^4 w}{\partial x^2 \partial t^2} + \rho A \frac{\partial^2 w}{\partial t^2} - F_x \left(\frac{\partial w}{\partial x} \right)^2 = f(x, t) \tag{12}$$

The identical analysis performed for the system without damping gives the characteristic equation:

$$EI(1 + 2i\mu\omega)s^4 + (\rho I\omega^2 - F_x)s^2 - \rho A\omega^2 = 0 \tag{13}$$

The solution (13) is four complex roots:

$$s_{1,2} = \pm i \sqrt{(\rho I - F_x) \frac{\omega^2}{2} + \omega \sqrt{I \frac{\rho^2 \omega^2}{4} + \rho A}} / 2EI(1 + 2i\mu\omega) \tag{14}$$

and

$$s_{1,2} = \pm \sqrt{-(\rho I - F_x) \frac{\omega^2}{2} + \omega \sqrt{I \frac{\rho^2 \omega^2}{4} + \rho A}} / 2EI(1 + 2i\mu\omega) \tag{15}$$

The analysis of the position of the elements on the plane of complex variables (Fig. 2) shows that some group of them is responsible for the generation of poorly damped vibrations. Another group of roots generates damped vibrations of the average frequency, and the next one introduces a structural delay to the system. Roots which lie on the real axis, and have large, negative values are usually omitted (inertial components).

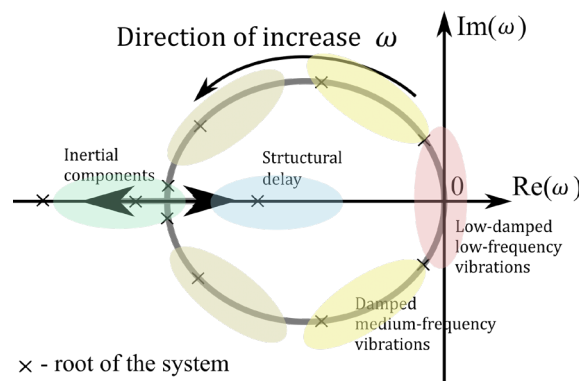


Figure 2. Distribution of the roots of the model on the plane of the complex variable- the location of complex and real elements.

The roots clustered close to each other and lying on the real correspond to inertial transmittances, the approximate model of which is the equivalent structural delay. Its value depends on the arm geometry, material parameters, and the axial force. It should be noted that for the increasing force $F_x > 0$, the elements reduce their imaginary part, which corresponds to the reduction in vibration amplitude. Some of the complex roots move to the real axis, see Fig. 3. The system loses its oscillating properties at higher frequencies but strengthens the structural delay.

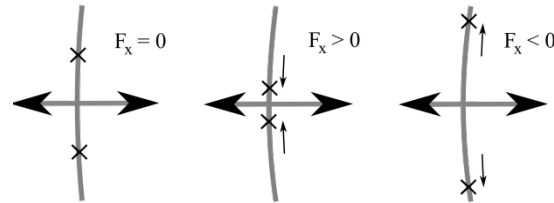


Figure 3. Distribution of the roots of the model on the plane of the complex variable- displacement of elements depending on the force F_x .

The reverse is the case for $F_x < 0$. The system tends to increase the oscillation (amplitude) at the expense of structural delays. The important conclusion is that the direction of the light-weight arm motion affects the amount of deformation. Even more important is the shape of distribution of the elements on the plane of the complex variable from the point of view of the control system synthesis task [7]. Even if the actual values are slightly different from the theoretical values, the principle of their mutual location will remain unchanged. For the limit values of material and geometric parameters, the area of their location is shown in Fig. 4.

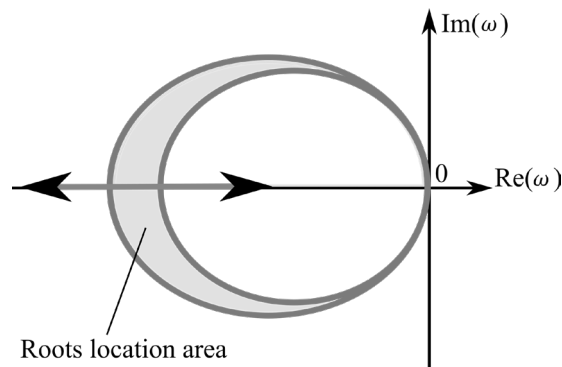


Figure 4. Area of the location of the elements on the plane of the complex variable.

As the distribution of elements for the three models: EBM, TM, and RM are similar, taking into account the degree of complication and the accuracy of the model, the approach with the use of RDFM seems to be the most advantageous solution.

4. Case study

We consider a planar system of two arms connected by rotary hinged joints, the lower of which is rigid and the upper is flexible (see Fig. 5).

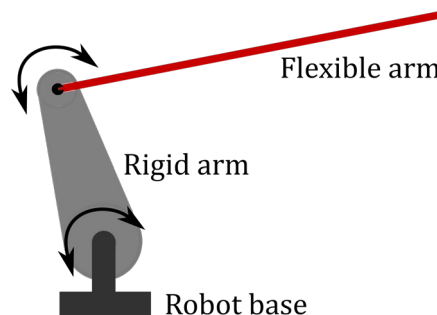


Figure 5. Planar system with two arms

Flexible arm parameters are shown in Table 2.

Table 2. Model parameters.

Parameter	Symbol	Unit	Value
Length of the arm	l	m	1.0
Density of the arm	ρ	kg/m ³	2700
Young's modulus of the arm	E	GPa	75
Inertia of cross-section of the arm	I	m ⁴	3.22e-9
Cross sectional area of the arm	A	m ²	2.011e-4
Damping coefficient of the arm	μ	1/s	4.5e-5

The dynamic properties of the system described in paragraphs two and three of the publication are clearly visible during the phases of the javelin-like motion. Figure 6a shows the phase of linear acceleration of the flexible arm under the influence of the force from the rigid arm. Figure 6b shows the phase for $F_x = 0$, it is the neutral state. Figure 6c shows the case where the linear motion of a flexible arm is decelerated.

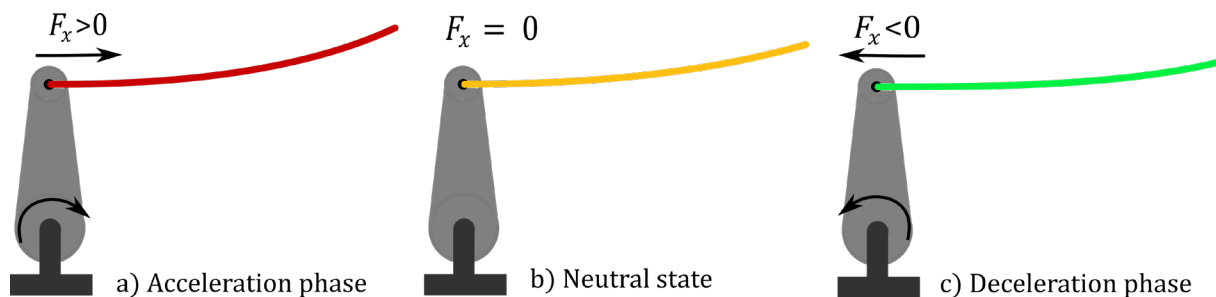


Figure 6. Three phases of motion of the flexible arm.

The three phases of motion shown in Fig. 6 correspond to the time series from Fig. 7. One can clearly see the influence of the axial force F_x on the system.

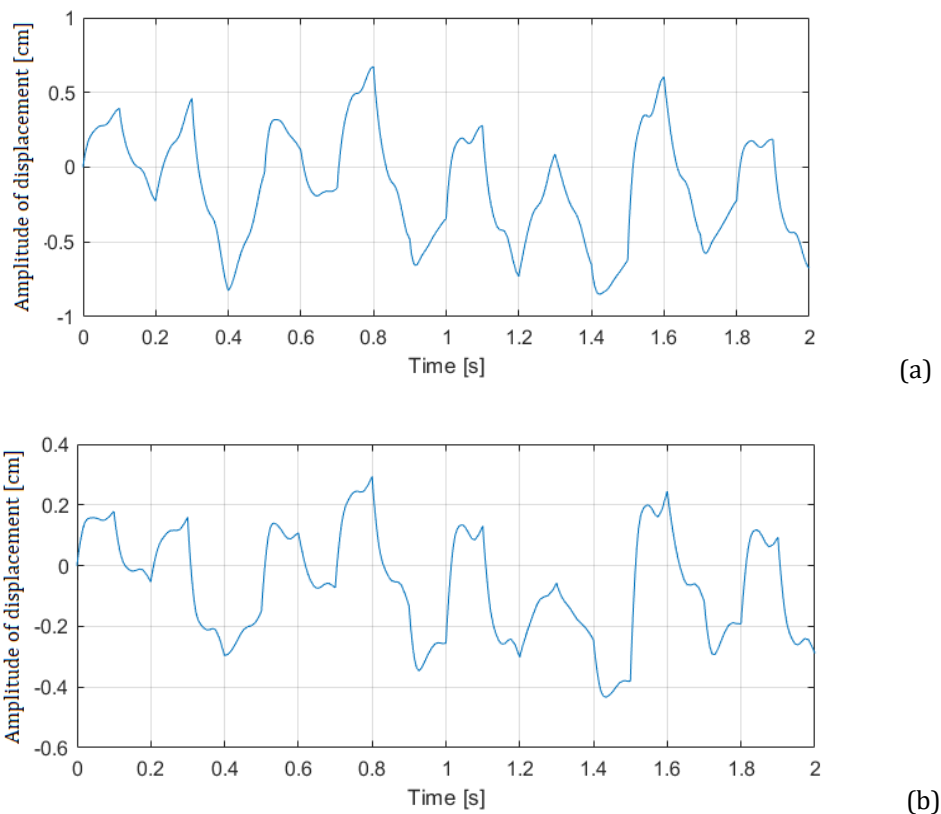


Figure 7. Time series of displacement amplitude during two phases of motion: (a) acceleration, (b) deceleration.

The maximum amplitude of vibrations in the acceleration phase is more than twice as large as the maximum amplitude of vibrations in the braking phase. This is an extremely unfavourable phenomenon that must be taken into account and then compensated by a sophisticated control system.

5. Conclusions

The paper describes selected problems related to the deformation of light robot arms and mathematical modelling of such structures, based on the knowledge resulting from the analysis of numerous publications and the author's own experience. Attention was focused on determining the position of the poles for three different models of transverse vibrations of the robot arm in the form of a beam. The three models considered are the Euler-Bernoulli model, the Rayleigh model, and the Timoshenko model with identical boundary conditions (clamped-free). Taking into account the accuracy of the model while maintaining the relative simplicity, the following analysis was carried out for the Rayleigh model enriched with the internal effect of structural viscoelasticity and the axial forces occurring in the arms during the acceleration and braking phase. It has been shown how strong is the influence of axial forces on the dynamic properties of the system. Taking into account the acceleration phase for an unfavourable arm configuration, the system may lose stability in rare cases.

Additional information

The authors declare: no competing financial interests and that all material taken from other sources (including their own published works) is clearly cited and that appropriate permits are obtained.

References

1. F. Axia, P. Trompette; Modeling of Mechanical Systems, Structural Elements; Elsevier 2005.
2. M. Geradin, D. Rixen; Mechanical vibrations- theory and application to structural dynamics; Wiley 1997.
3. C. Felippa; The Amusing History of Shear Flexible Beam Elements, Report No. CU-CAS-05-1, University of Colorado, 2005.

4. O. C. Zienkiewicz, R. L. Taylor; The Finite Element Method; Oxford 2000.
5. S.M. Han, H. Benaroya, T. Wei; Dynamics of Transversely Vibrating Beams using Four Engineering Theories; Journal of Sound and Vibration, 1999, 225(5), 935-988.
6. P. Arbenz; Lecture Notes on Solving Large Scale Eigenvalue Problems; Computer Science Department ETH Zurich, 2016.
7. R. Leniowski, L. Leniowska; The multi-segment controller of a flexible arm; ISR 2020; 52th International Symposium on Robotics, VDE Verlag, 2020, 1-8. ISBN:978-3-8007-5428-1.
8. W.J. Book; Recursive Lagrangian dynamics of flexible manipulator arms; Int. Journal of Robotics Research, 1984, 3(3), 87-101.
9. S. S. Rao; Vibration of Continuous Systems; John Wiley & Sons, Inc., 2007. ISBN: 978-0-471-77171-5.
10. L. Majkut; Free and forced vibration of Timoshenko beams described by single difference equation; Journal of Theoretical and Applied Mechanics, 2009, 47(1), 193-210.

© 2022 by the Authors. Licensee Poznan University of Technology (Poznan, Poland). This article is an open access article distributed under the terms and conditions of the Creative Commons Attribution (CC BY) license (<http://creativecommons.org/licenses/by/4.0/>).